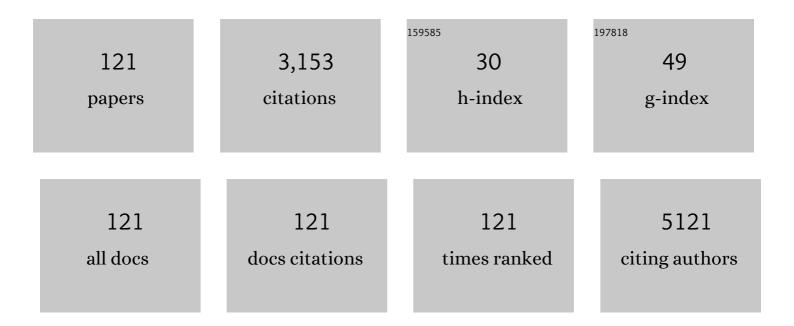
## Suklyun Hong

List of Publications by Year in descending order

Source: https://exaly.com/author-pdf/720071/publications.pdf Version: 2024-02-01



#	Article	IF	CITATIONS
1	Rapid chemical vapor deposition of graphene using methanol as a precursor. Carbon Letters, 2021, 31, 307-313.	5.9	6
2	Electronic structure of graphene/Y2C heterostructure and related doping effect. Current Applied Physics, 2021, 28, 13-18.	2.4	5
3	Indium-contacted van der Waals gap tunneling spectroscopy for van der Waals layered materials. Scientific Reports, 2021, 11, 17790.	3.3	1
4	Substrate effect on doping and degradation of graphene. Carbon, 2021, 184, 651-658.	10.3	8
5	Effect of Point Defects on Electronic Structure of Monolayer GeS. Nanomaterials, 2021, 11, 2960.	4.1	2
6	Effect of atomic passivation at Ni-MoS2 interfaces on contact behaviors. Current Applied Physics, 2020, 20, 132-136.	2.4	5
7	Transport gaps in ideal zigzag-edge graphene nanoribbons with chemical edge disorder. Applied Surface Science, 2020, 512, 144714.	6.1	5
8	Thicknessâ€Dependent, Gateâ€Tunable Rectification and Highly Sensitive Photovoltaic Behavior of Heterostructured GeSe/WS <sub>2</sub> p–n Diode. Advanced Materials Interfaces, 2020, 7, 2000893.	3.7	25
9	Selective-Area Remote Epitaxy of ZnO Microrods Using Multilayer–Monolayer-Patterned Graphene for Transferable and Flexible Device Fabrications. ACS Applied Nano Materials, 2020, 3, 8920-8930.	5.0	25
10	Adsorption of Acetonitrile on Si(111)-(7 × 7). ACS Omega, 2020, 5, 24179-24185.	3.5	3
11	Understanding filamentary growth and rupture by Ag ion migration through single-crystalline 2D layered CrPS4. NPG Asia Materials, 2020, 12, .	7.9	9
12	Remote heteroepitaxy of GaN microrod heterostructures for deformable light-emitting diodes and wafer recycle. Science Advances, 2020, 6, eaaz5180.	10.3	80
13	One-dimensional hexagonal boron nitride conducting channel. Science Advances, 2020, 6, eaay4958.	10.3	37
14	Contact properties of 2D/3D GaSe/Si(1Â1Â1) heterostructure. Applied Surface Science, 2020, 516, 145969.	6.1	3
15	Monolithic Interface Contact Engineering to Boost Optoelectronic Performances of 2D Semiconductor Photovoltaic Heterojunctions. Nano Letters, 2020, 20, 2443-2451.	9.1	31
16	In-Depth Structural Characterization of 1T-VSe <sub>2</sub> Single Crystals Grown by Chemical Vapor Transport. Crystal Growth and Design, 2020, 20, 2860-2865.	3.0	21
17	3D graphene-cellulose nanofiber hybrid scaffolds for cortical reconstruction in brain injuries. 2D Materials, 2019, 6, 045043.	4.4	14
18	Tailoring Surface Properties via Functionalized Hydrofluorinated Graphene Compounds. Advanced Materials, 2019, 31, e1903424.	21.0	23

#	Article	IF	CITATIONS
19	Investigation of atomic and electronic properties of 2D-MoS <sub>2</sub> /3D-GaN mixed-dimensional heterostructures. Nanotechnology, 2019, 30, 404002.	2.6	12
20	Effects of intercalated atoms on electronic structure of graphene nanoribbon/hexagonal boron nitride stacked layer. Scientific Reports, 2019, 9, 3623.	3.3	2
21	Significant THz absorption in CH3NH2 molecular defect-incorporated organic-inorganic hybrid perovskite thin film. Scientific Reports, 2019, 9, 5811.	3.3	26
22	Layer dependent electrical transport in exfoliated graphene FETs under UV illumination. Applied Surface Science, 2019, 479, 863-873.	6.1	2
23	Black Phosphorus-IGZO van der Waals Diode with Low-Resistivity Metal Contacts. ACS Applied Materials & Interfaces, 2019, 11, 10959-10966.	8.0	31
24	Rapid synthesis of graphene by chemical vapor deposition using liquefied petroleum gas as precursor. Carbon, 2019, 145, 462-469.	10.3	23
25	Surface Instability of Sn-Based Hybrid Perovskite Thin Film, CH <sub>3</sub> NH <sub>3</sub> SnI <sub>3</sub> : The Origin of Its Material Instability. Journal of Physical Chemistry Letters, 2018, 9, 2293-2297.	4.6	45
26	Controlled Electrochemical Intercalation of Graphene/ <i>h-</i> BN van der Waals Heterostructures. Nano Letters, 2018, 18, 460-466.	9.1	49
27	Thermodynamic design of a high temperature chemical vapor deposition process to synthesize α-SiC in Si-C-H and Si-C-H-Cl systems. Journal of Crystal Growth, 2018, 485, 78-85.	1.5	8
28	Temperature-Dependent and Gate-Tunable Rectification in a Black Phosphorus/WS <sub>2</sub> van der Waals Heterojunction Diode. ACS Applied Materials & Interfaces, 2018, 10, 13150-13157.	8.0	61
29	Van der Waals heterojunction diode composed of WS <sub>2</sub> flake placed on p-type Si substrate. Nanotechnology, 2018, 29, 045201.	2.6	21
30	Mixed-dimensional 2D/3D heterojunctions between MoS <sub>2</sub> and Si(100). Physical Chemistry Chemical Physics, 2018, 20, 25240-25245.	2.8	7
31	Remote homoepitaxy of ZnO microrods across graphene layers. Nanoscale, 2018, 10, 22970-22980.	5.6	33
32	Remote heteroepitaxy across graphene: Hydrothermal growth of vertical ZnO microrods on graphene-coated GaN substrate. Applied Physics Letters, 2018, 113, .	3.3	30
33	Ab initio study of adsorption behaviors of molecular adsorbates on the surface and at the edge of MoS 2. Current Applied Physics, 2018, 18, 1013-1019.	2.4	18
34	Functionalization of Ge(1 0 0) surface by adsorption of phenylthiol. Applied Surface Science, 2018, 456, 908-914.	6.1	2
35	Van der Waals Density Functional Theory Study of Molecular Adsorbates on MoX2(X = S, Se or Te). Journal of the Korean Physical Society, 2018, 73, 100-104.	0.7	14

<sup>36</sup> Ferromagnetic contact between Ni and MoX <sub>2</sub> (X  =  S, Se, or Te) with Fermi-level pinning. 2D<sub>28</sub> Materials, 2017, 4, 024006.

#	Article	IF	CITATIONS
37	Edge-functionalization of armchair graphene nanoribbons with pentagonal-hexagonal edge structures. Journal of Physics Condensed Matter, 2017, 29, 245301.	1.8	2
38	Systematic study of electronic structure and band alignment of monolayer transition metal dichalcogenides in Van der Waals heterostructures. 2D Materials, 2017, 4, 015026.	4.4	160
39	A first-principles study on the adsorption of ethylenediamine on Ge(100). Physical Chemistry Chemical Physics, 2017, 19, 16881-16887.	2.8	4
40	Band Alignment at Au/MoS <sub>2</sub> Contacts: Thickness Dependence of Exfoliated Flakes. Journal of Physical Chemistry C, 2017, 121, 22517-22522.	3.1	34
41	Point defects in turbostratic stacked bilayer graphene. Nanoscale, 2017, 9, 13725-13730.	5.6	12
42	Reduction of Fermi level pinning at Au–MoS <sub>2</sub> interfaces by atomic passivation on Au surface. 2D Materials, 2017, 4, 015019.	4.4	40
43	Strain-induced non-linear optical characteristics of pyroelectric PbVO_3 epitaxial thin films. Optical Materials Express, 2017, 7, 62.	3.0	5
44	Investigations of Vacancy Structures Related to Their Growth in h-BN Sheet. Nanoscale Research Letters, 2017, 12, 445.	5.7	23
45	The presence of CH3NH2 neutral species in organometal halide perovskite films. Applied Physics Letters, 2016, 108, .	3.3	50
46	<i>In Situ</i> Atomic Level Dynamics of Heterogeneous Nucleation and Growth of Graphene from Inorganic Nanoparticle Seeds. ACS Nano, 2016, 10, 9397-9410.	14.6	11
47	Charge Mediated Reversible Metal–Insulator Transition in Monolayer MoTe <sub>2</sub> and W <sub><i>x</i></sub> Mo <sub>1–<i>x</i></sub> Te <sub>2</sub> Alloy. ACS Nano, 2016, 10, 7370-7375.	14.6	133
48	Observation of graphene grain boundaries through selective adsorption of rhodamine B using fluorescence microscopy. Carbon, 2016, 108, 72-78.	10.3	3
49	High-throughput screening of metal-porphyrin-like graphenes for selective capture of carbon dioxide. Scientific Reports, 2016, 6, 21788.	3.3	31
50	Energy Bandgap and Edge States in an Epitaxially Grown Graphene/h-BN Heterostructure. Scientific Reports, 2016, 6, 31160.	3.3	19
51	Theoretical Demonstration of the Ionic Barristor. Nano Letters, 2016, 16, 2090-2095.	9.1	9
52	Electronic Properties of Bilayer Graphene Strongly Coupled to Interlayer Stacking and an External Electric Field. Physical Review Letters, 2015, 115, 015502.	7.8	47
53	Phase stability of transition metal dichalcogenide by competing ligand field stabilization and charge density wave. 2D Materials, 2015, 2, 035019.	4.4	29
54	In situ hybridization of carbon nanotubes with bacterial cellulose for three-dimensional hybrid bioscaffolds. Biomaterials, 2015, 58, 93-102.	11.4	82

#	Article	IF	CITATIONS
55	Effect of Annealing in Ar/H <sub>2</sub> Environment on Chemical Vapor Deposition-Grown Graphene Transferred With Poly (Methyl Methacrylate). IEEE Nanotechnology Magazine, 2015, 14, 70-74.	2.0	34
56	Van der Waals density functional theory study for bulk solids with BCC, FCC, and diamond structures. Current Applied Physics, 2015, 15, 885-891.	2.4	43
57	Doping effect in graphene on oxide substrates: MgO(111) and SiO2(0001). Current Applied Physics, 2015, 15, S103-S107.	2.4	6
58	Atomic-scale dynamics of triangular hole growth in monolayer hexagonal boron nitride under electron irradiation. Nanoscale, 2015, 7, 10600-10605.	5.6	63
59	Ab initio study of adsorption properties of hazardous organic molecules on graphene: Phenol, phenyl azide, and phenylnitrene. Chemical Physics Letters, 2015, 618, 57-62.	2.6	26
60	Indirect-direct band gap transition through electric tuning in bilayer MoS2. Journal of Chemical Physics, 2014, 140, 174707.	3.0	40
61	Graphene oxide catalyzed cis-trans isomerization of azobenzene. APL Materials, 2014, 2, .	5.1	7
62	Spatial variation in the electronic structures of carpetlike graphene nanoribbons and sheets. Current Applied Physics, 2014, 14, 1687-1691.	2.4	1
63	First-principles study of carbon atoms adsorbed on MgO(100) related to graphene growth. Current Applied Physics, 2013, 13, 327-330.	2.4	27
64	Modification of Electrical Properties of Graphene by Substrate-Induced Nanomodulation. Nano Letters, 2013, 13, 3494-3500.	9.1	94
65	Polar oxide substrates for graphene growth: A first-principles investigation of graphene on MgO(111). Current Applied Physics, 2013, 13, 803-807.	2.4	13
66	Thermally Induced Desulfurization: Structural Transformation of Thiophene on the Si(100) Surface. Journal of Physical Chemistry C, 2013, 117, 11731-11737.	3.1	9
67	Ab initio Investigations of Carbon Atoms Adsorbed on α-Al2O3 Surfaces in Relation to Graphene Growth. Journal of the Physical Society of Japan, 2013, 82, 114709.	1.6	2
68	Adsorption and Surface Diffusion of Pt Atoms on Hydroxylated MgO(001) Surfaces. Journal of the Physical Society of Japan, 2013, 82, 034603.	1.6	16
69	Ab-initio Study of Interactions of Gold Atoms with Hydroxylated MgO(001) Surfaces. Journal of the Physical Society of Japan, 2012, 81, 054601.	1.6	17
70	Enhanced binding strength between metal nanoclusters and carbon nanotubes with an atomic nickel defect. Nanotechnology, 2012, 23, 205204.	2.6	11
71	Effect of charge-transfer complex on the energy level alignment between graphene and organic molecules. Applied Physics Letters, 2012, 100, 183102.	3.3	5
72	Adsorption Structure and Reaction Mechanism of Purine on Ge(100) Studied by Scanning Tunneling Microscopy and Theoretical Calculations. Journal of Physical Chemistry C, 2012, 116, 6953-6959.	3.1	12

#	Article	IF	CITATIONS
73	Graphitic Carbon Growth on MgO(100) by Molecular Beam Epitaxy. Journal of Physical Chemistry C, 2012, 116, 7380-7385.	3.1	23
74	Structure of Glycine on Ge(100): Ab Initio Study of Its Scanning Tunneling Microscopy Images. Journal of Physical Chemistry C, 2012, 116, 13890-13895.	3.1	2
75	First-principles study of substitutional carbon pair and Stone–Wales defect complexes in boron nitride nanotubes. Chemical Physics Letters, 2012, 522, 79-82.	2.6	20
76	Enhanced Deseleniumization of Selenophene Molecules Adsorbed on Si(100)-2 × 1 Surface. Journal of Physical Chemistry C, 2011, 115, 17856-17860.	3.1	4
77	Nanocrystalline Graphite Growth on Sapphire by Carbon Molecular Beam Epitaxy. Journal of Physical Chemistry C, 2011, 115, 4491-4494.	3.1	113
78	Hydrogen-Bonded Amino Acid Network of Histidine on Ge(100). Journal of Physical Chemistry C, 2011, 115, 4636-4641.	3.1	15
79	Atomic and electronic structure of styrene on Ge(100). Surface Science, 2011, 605, 1438-1444.	1.9	3
80	Origins of dihydrogen binding to metal-inserted porphyrins: Electric polarization and Kubas interaction. Journal of Chemical Physics, 2011, 134, 234701.	3.0	6
81	Ab initio Calculations with van der Waals Corrections: Benzene-benzene Intermolecular Case and Graphite. Journal of the Korean Physical Society, 2011, 59, 196-199.	0.7	18
82	Atomic and electronic structure of methanol on Ge(100). Surface Science, 2010, 604, 129-135.	1.9	22
83	Monovacancy and substitutional defects in hexagonal silicon nanotubes. Solid State Communications, 2009, 149, 408-411.	1.9	4
84	Ab initio study of hydrogen binding on Ca-inserted porphyrin. Vacuum, 2009, 84, 537-539.	3.5	5
85	Discrimination of Chiral Adsorption Configurations: Styrene on Germanium(100). Journal of Physical Chemistry C, 2009, 113, 1426-1432.	3.1	10
86	Realistic adsorption geometries and binding affinities of metal nanoparticles onto the surface of carbon nanotubes. Applied Physics Letters, 2009, 94, .	3.3	27
87	Hydrogen adsorption on hexagonal silicon nanotubes. Solid State Communications, 2008, 148, 469-471.	1.9	20
88	Carbon diffusion around the edge region of nickel nanoparticles. Applied Physics Letters, 2008, 92, 043103.	3.3	22
89	Atomic and Electronic Structure of Pyrrole on Ge(100). Journal of Physical Chemistry C, 2008, 112, 7412-7419.	3.1	17
90	Dissociative Chemisorption of Methanol on Ge(100). Journal of Physical Chemistry C, 2007, 111, 15013-15019.	3.1	37

#	Article	IF	CITATIONS
91	Bidentate Structures of Acetic Acid on Ge(100):  The Role of Carboxyl Oxygen. Journal of Physical Chemistry C, 2007, 111, 5941-5945.	3.1	23
92	Computational Study of Hydrogen Storage Characteristics of Covalent-Bonded Graphenes. Journal of the American Chemical Society, 2007, 129, 8999-9003.	13.7	161
93	Chemical Reactions and Adsorption Geometries of Pyrrole on Ge(100). Journal of Physical Chemistry B, 2006, 110, 7938-7943.	2.6	13
94	Theoretical STM images of alkaline-earth metal adsorbed Si(111)3×2 surfaces. Surface Science, 2006, 600, 3606-3609.	1.9	7
95	Atomic and electronic structure of acetic acid on Ge(100). Surface Science, 2006, 600, 3629-3632.	1.9	19
96	Structure of Pyrrole on Ge(100). Japanese Journal of Applied Physics, 2006, 45, 2148-2150.	1.5	2
97	Ab initio study of the effect of water adsorption on the carbon nanotube field-effect transistor. Applied Physics Letters, 2006, 89, 243110.	3.3	63
98	Metallization of the semiconducting carbon nanotube by encapsulated bromine molecules. Physica E: Low-Dimensional Systems and Nanostructures, 2005, 29, 693-697.	2.7	14
99	Double Dative Bond Configuration:Â Pyrimidine on Ge(100). Journal of Physical Chemistry B, 2005, 109, 348-351.	2.6	40
100	Study of Adsorption and Decomposition of H2O on Ge(100). Journal of Physical Chemistry B, 2005, 109, 24445-24449.	2.6	24
101	Electronic structure calculations of metal-nanotube contacts with or without oxygen adsorption. Physical Review B, 2005, 72, .	3.2	39
102	Effect of Hydrogen on Carbon Diffusion on Ni(111). Japanese Journal of Applied Physics, 2004, 43, 773-774.	1.5	6
103	Atomic and Electronic Structure of Pyridine on Ge(100). Journal of Physical Chemistry B, 2004, 108, 15229-15232.	2.6	30
104	Surface energy anisotropy of iron surfaces by carbon adsorption. Current Applied Physics, 2003, 3, 457-460.	2.4	26
105	Formation of Highly Ordered Organic Monolayers by Dative Bonding:Â Pyridine on Ge(100). Journal of the American Chemical Society, 2003, 125, 7514-7515.	13.7	61
106	Energetics of the dihydride phases on the diamond (100) surface. Physical Review B, 2002, 65, .	3.2	7
107	First-Principles Study of Atomic and Electronic Structure of Ba/Si(111). Journal of the Physical Society of Japan, 2002, 71, 2761-2764.	1.6	6
108	Crystal Shape of a Nickel Particle Related to Carbon Nanotube Growth. Japanese Journal of Applied Physics, 2002, 41, 6142-6144.	1.5	41

#	ARTICLE	IF	CITATIONS
109	Theoretical study on cracking behavior in two-phase alloys Cr–Cr2X (X=Hf, Nb, Ta, Zr). Intermetallics, 2001, 9, 799-805.	3.9	24
110	Structure of the Ba-InducedSi(111)-(3×2)Reconstruction. Physical Review Letters, 2001, 87, 056104.	7.8	64
111	First-principles calculation of stacking fault and twin boundary energies of Cr2Nb. Philosophical Magazine A: Physics of Condensed Matter, Structure, Defects and Mechanical Properties, 2000, 80, 871-880.	0.6	13
112	Phase stability and elastic moduli of Cr2Nb by first-principles calculations. Intermetallics, 1999, 7, 5-9.	3.9	93
113	Elastic properties and stacking fault energies of Cr2Ta. Intermetallics, 1999, 7, 1169-1172.	3.9	26
114	Role of hydrogen inSiH2adsorption on Si(100). Physical Review B, 1998, 58, R13363-R13366.	3.2	20
115	Effect of hydrogen on the surface-energy anisotropy of diamond and silicon. Physical Review B, 1998, 57, 6262-6265.	3.2	56
116	Theoretical study of hydrogen-covered diamond (100) surfaces: A chemical-potential analysis. Physical Review B, 1997, 55, 9975-9982.	3.2	38
117	Correlation energy and its temperature dependence. Physical Review B, 1996, 53, 1215-1224.	3.2	4
118	Temperature dependence of the Hartree-Fock approximation in two dimensions. Physical Review B, 1995, 52, 7860-7863.	3.2	7
119	Spin-polarized Hartree-Fock approximation at nonzero temperatures. Physical Review B, 1995, 51, 17417-17430.	3.2	3
120	Temperature dependence of the Hartree-Fock approximation. Physical Review B, 1994, 50, 7284-7290.	3.2	8
121	Conserving approximations: Electron gas with exchange effects. Physical Review B, 1994, 50, 8182-8188.	3.2	12